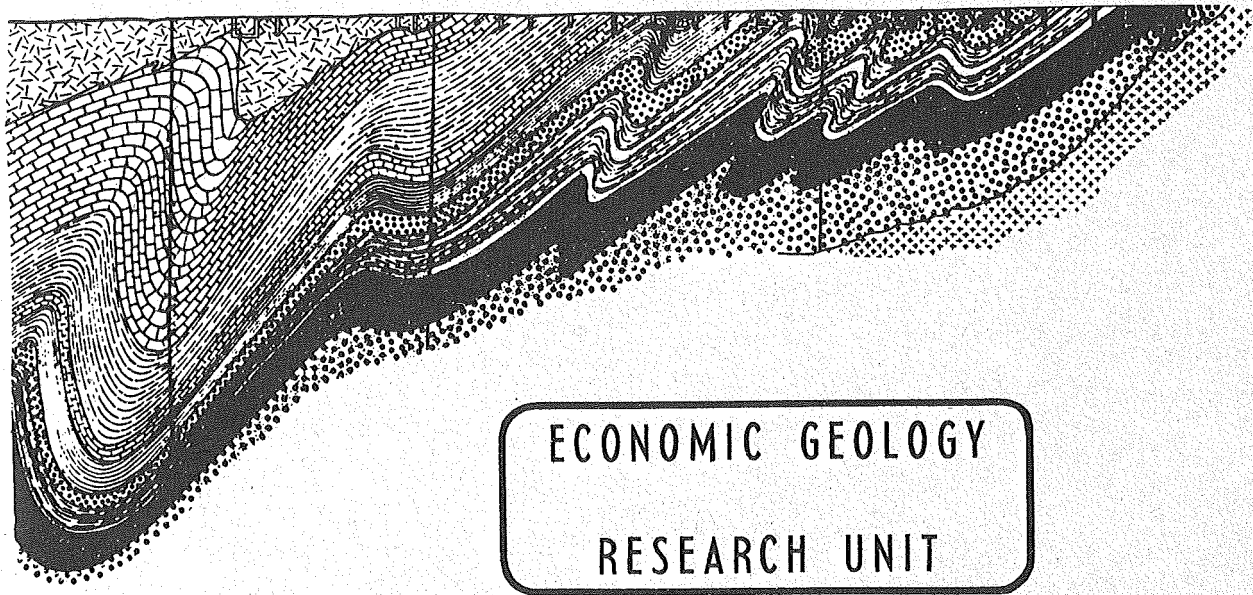




UNIVERSITY OF THE WITWATERSRAND
JOHANNESBURG



INFORMATION CIRCULAR No. 46

NON-OROGENIC GRANITES AND THE AGE OF
THE PRECAMBRIAN PONGOLA SEQUENCE

C. ROERING

UNIVERSITY OF THE WITWATERSRAND

JOHANNESBURG

NON-OROGENIC GRANITES AND THE AGE OF
THE PRECAMBRIAN PONGOLA SEQUENCE

by

C. ROERING

(Research Fellow, Economic Geology Research Unit)

ECONOMIC GEOLOGY RESEARCH UNIT

INFORMATION CIRCULAR No. 46

May, 1968

NON-OROGENIC GRANITES AND THE AGE OF
THE PRECAMBRIAN PONGOLA SEQUENCE

ABSTRACT

Portion of the Pongola Sequence (comprising an andesitic lava group overlain by a succession of quartzites, conglomerates, and shales) occurring in the southwestern part of Swaziland has been studied with a view to obtaining the age relationships of the folding, metamorphism, and intrusion of G.4 and G.5 granites. These granites are of prime interest because of their great ages, the minima of which are 3,050 m.y. and 2,600 m.y. These varieties are similar to other intrusive basement granites of South Africa, and are possibly associated with a differentiative process in the mantle, rather than with conventional geo-synclinal agencies. The ages of the intrusive granites indicate that the Pongola Sequence is older than the Dominion Reef Group at the base of the Witwatersrand Sequence. Previously accepted ideas on the Pongola rocks being correlatives of Witwatersrand strata can now be dismissed as invalid.

Five distinct ages of deformation have been identified in the supracrustal rocks. The first two periods (S_1 and S_2), which cannot be distinguished as they are so closely oriented, resulted in folds about north-south-trending axes. The main structure developed was a syncline which was folded by later S_3 folds along a northeast trend. Refolding resulted in the original syncline being buckled into two subsidiary synclines, one plunging to the north, the other towards the south. The fourth phase of deformation was not accompanied by the development of any large folds, but was responsible for a prominent schistosity which has a dip of 30° to the northwest. Numerous minor folds and lineations were produced during this deformational period. The final phase is represented by the reactivation of the previously passively-behaved bedding planes as thrust surfaces. Thrusting was responsible for the overlying beds being transported from east to west.

The contact phase of the intrusive G.4 granite, on petrofabric analysis, reveals a well-developed biotite girdle in every locality investigated. Examination of the girdles shows that this granite was responsible for the metamorphism of the supracrustal rocks, and yet was itself involved in the important deformational phases. Petrofabric analysis of the G.5 granite proves that it is unrelated to the folding, and is thus post-folding in age.

The metamorphism in the area reflects an increasing grade towards the granite contact. Andalusite is developed farthest away from the granite, while close to it sillimanite is developed. The metamorphism was initiated during, and prior to, the S_1 and S_2 period of deformation.

Zircon studies from the two granites reveal two distinct populations, and suggest that the G.5 granite was essentially magmatic, while the G.4 may not have reached such a progressive state of magmatism.

* * * * *

NON-OROGENIC GRANITES AND THE AGE OF
THE PRECAMBRIAN PONGOLA SEQUENCE

CONTENTS

	<u>Page</u>
<u>INTRODUCTION</u>	1
A. Location and Geological Setting	1
B. Previous Work	1
C. Aims of the Present Investigation	4
<u>THE METAMORPHIC ROCK ASSEMBLAGE</u>	4
A. Metamorphosed Insuzi Rocks	5
B. Metamorphosed Mozaan Rocks	5
C. Significance of the Metamorphic Assemblages	6
<u>THE INTRUSIVE GRANITES AND DYKES</u>	7
A. The G.4 Granite	7
B. The G.5 Granite	8
C. Zircons from the Granites	8
D. Dykes	10
<u>STRUCTURAL GEOLOGY</u>	10
A. Major Structures	10
B. Analysis of Data on Minor Structures	10
C. Petrofabric Analyses of the G.4 and G.5 Granites	13
<u>THE AGE OF THE PONGOLA SEQUENCE</u>	14
<hr/>	
List of References Cited	16
Key to Figures	18

* * * * *

NON-OROGENIC GRANITES AND THE AGE OF THE PRECAMBRIAN PONGOLA SEQUENCE

INTRODUCTION

A. LOCATION AND GEOLOGICAL SETTING

The area investigated, which is approximately 15 square miles in extent, lies in the southwestern portion of Swaziland, some 11 miles southeast of Mankalana. It is situated between the Ngwempisi and Mkhondo (Assegai) rivers, at a distance of five miles from both. The smaller Mozane River lies seven miles to the south of the area, the coordinates of which are :

26°45'S — 26°48'S Latitudes
31°09'E — 31°14'E Longitudes

The area mapped occurs at the northern end of the Mahlangatsha Plateau, which has a mean elevation of 4,200 feet, and is somewhat rugged in character. Making up the plateau are Upper Pongola rocks consisting of alternating harder and softer schists, derived from quartzites and shales, which have weathered to produce a series of ridges with intervening lower and flatter portions. In the west, the Lower Pongola lava sequence produces a much softer type of topography. Towards the north and northwest, the plateau ends abruptly against the G.5 granite. The latter has weathered to form a hilly topography, which is broken locally by granite tors, and which has a lower mean elevation (3,200—3,700 feet) than the Mahlangatsha Plateau.

B. PREVIOUS WORK

The earliest work of significance relating to the area was carried out to the southwest of Mahlangatsha by Humphrey and Krige (1931) who mapped and described the geology of the country south of Plet Retlef. They classified the Pongola Sequence as consisting of a Lower Group, which comprises 16,000 feet of lavas, 3,000 feet of quartzites, and a few hundred feet of phyllite, and an Upper Group of alternating quartzites and shales, 16,000 feet thick, with one thin bed of lava.

Humphrey and Krige (1931) reported that the granite found within the area is intrusive into the Pongola Sequence. However, in the west, the Lower Pongola Group was seen to be separated from the granite by a zone of intrusive gabbro and granophyre along a larger part of its base. On the farm Warmbad, they found that the Lower Pongola Warmbad quartzite shows "..... no signs of contact metamorphism and the field evidence there is in favour of a sedimentary contact. But this evidence does not seem conclusive". In this regard, they quoted du Toit (1931), who, in his mapping of the Nkandla area, found that the Insuzi Group (Lower Pongola) rests upon an older granite with a sedimentary contact. In an appendix, Humphrey and Krige (1931) suggested that the lowermost members of the Warmbad Quartzite had been thermally metamorphosed, from which it followed that the intrusive nature of the "..... eastern and western contacts of the granites and the Pongola beds may be therefore regarded as having been established".

The granite of the Plet Retlef area is variable in type. The most common variety is a coarse-grained grey granite with muscovite and biotite. Hornblende may take the place of the latter mineral. Acid veins are frequently found traversing the granite, while very basic patches are also encountered. The conclusion was drawn by Humphrey and Krige (1931) that "..... it is reasonable to assume that granite of only one age is represented, namely the Old Granite of the Transvaal". On this evidence, they correlated the Upper

Pongola Group with the Moodies Group, and the Lower Pongola Group with the Onverwacht Group of the Swaziland Sequence of the Barberton Mountain Land, as classified by Hall (1918).

The suggested correlation of Humphrey and Krige (1931) was rejected by Hamilton (1938a and b). In examining the rocks of the Kubuta area of Swaziland, he concluded that there are two granites of widely different age. There is a pre-Pongola granite and gneiss, as well as a post-Pongola red granite with "Bushveld Granite similarities". The Upper Pongola Group was consequently correlated with the Witwatersrand Sequence. The correlation of Humphrey and Krige (1931) was also discarded because of the "..... highly folded nature of the Moodies beds in the Barberton area (and) the comparatively gentle synclinal basin structure of the Pongola beds". It should be noted that the post-Pongola granite described by Hamilton (1938b) is a leucocratic biotite granite "and of remarkably uniform composition and texture. It lacks any directive textures and apparently also pegmatites". This same granite was classified as G.5 by Hunter (1961).

Mehliss (1961) mapped the Mahlangatsha area in 1946. He recognised a Lower Pongola Group of lavas with rather erratic intercalations of quartzite and phyllite, and an Upper Group of sediments. He noted that the Upper Pongola rocks have suffered metamorphism. Although he found the Pongola beds to be older than the granites in the area, Mehliss (1961) correlated the Pongola Sequence with the Witwatersrand Sequence, including the Dominion Reef Group. However, he agreed that the Lower Witwatersrand is younger than a granite which is similar to that found in the Mahlangatsha area. This difficulty was overcome by suggesting that "the Older granite is made up of various phases, which, while petrographically similar, were emplaced at widely separated periods of time".

Truter (1949) correlated the Lower Pongola, or Insuzi, Group with the Dominion Reef Group, stating that "The basal rocks rest with a sedimentary contact either on older granite or on a gabbro and an associated porphyritic granite intrusive into it. Intrusive into the Insuzi is an igneous complex composed of gabbro, gabbro-porphyry, microgranite and granophyre. The entire assemblage of sedimentary, extrusive and younger intrusive rocks is overlain unconformably by rocks of the Mozaan or Upper Pongola Series". Concerning the rocks of the Mozaan Group (Upper Pongola) which extends from Amsterdam in a southeasterly direction past Plet Retlef to beyond Louwsberg in Natal, Truter (1949) said: "In the east and south-east they rest on older granite while in the west and north-west they lie unconformably on rocks of the Insuzi Series". On these and other grounds, he correlated the Mozaan Group with the Witwatersrand Sequence. It should be noted that Truter (1949) apparently disregarded all previous investigations which recorded intrusive granite relationships.

Truter and Rossouw (1955) showed on the 1:1,000,000 geological map of the Republic of South Africa that they accepted an intrusive granitic relationship on the eastern side of the Mozaan Group in Swaziland. However, a thin margin of Moodies rocks was alleged to replace Mozaan rocks in the critical area where other investigators had found the effects of metamorphism associated with the intrusion of the eastern granites.

Hunter (1957) undertook an investigation of all the granites in Swaziland, and classified them into various groups, G.1 to G.5. The G.4 granite clearly intrudes the Insuzi and Mozaan Groups. The contact west of the Mkhondo River reveals small granite bodies emplaced in the Mozaan Group taking advantage of shale horizons. Pegmatites are found within the Pongola rocks up to five miles from the nearest exposed granite. Hunter (1957) concluded that the Mozaan Group might be older than the Witwatersrand Sequence, and clearly stated the need for age determinations of the various granites.

Matthews (1959), referring to the sedimentary contact that du Toit (1931) postulated for the base of the Insuzi Group in the Nkandla area, stated: "Although the transgressive contact mapped by du Toit was recognized the sedimentary unconformity

postulated by him was found on careful examination to be a concordant intrusive contact".

Hunter (1961), in describing the geology of Swaziland, stated that, due to the controversy over the correlation of the Pongola rocks, the non-committal terms Insuzi and Mozaan Series should be used: "The official view in Swaziland is that the correlation of these two series is open debate". What he referred to is the official view taken by the South African Geological Survey which, in 1955, correlated the Insuzi with the Dominion Reef Group and the Mozaan with the Witwatersrand Sequence. In the same paper, Hunter (1961) stated that the Mozaan rocks characteristically lack metamorphism, where intruded by any of the G.5 granite plutons. Other post-Mozaan granites show more marked effects. The G.4 granite often recrystallizes quartzites to material that resembles vein quartz. Various metamorphic minerals, found in the Mozaan near the G.4 granite, include andalusite, amphibole, garnet, and sillimanite.

Allsopp et al (1962), using the Sr-Rb method, have dated various Swaziland granites. The ages obtained from four total rock analyses of G.4 show that this granite was emplaced $3,070 \pm 60$ m.y. ago. The granite is clearly established as post-Mozaan in age, and therefore the Pongola Sequence must be older. The age of the Makungutsha G.5 pluton that intrudes the Mozaan rocks in the area described in the present paper is $2,880 \pm 340$ m.y.

Recent mapping by Winter (1963) shows that Mozaan in the Mahlangatsha area is intruded by both the G.4 and G.5 granites. The G.4 is responsible for the formation of staurolite schists, garnet-mica meta-quartzites, granulites, and sillimanite-bearing quartz schists. Large-scale fold structures in the Mozaan strata can be followed up to the contact of the G.4 granite, and the metamorphosed portions of these continuous structures certainly cannot be classified as Moodies rocks, as suggested by Truter and Rossouw (1955).

Most of the above work, plus unpublished information by Hunter and Winter on the Pongola Sequence in Swaziland, forms the basis of a paper by Hunter (1963) on the Mozaan Group. He reiterates that the Mozaan rocks are intruded by the G.4 and G.5 granites, and since the G.4 is dated as 3,070 m.y., the Mozaan Group must be older than this. From Winter's (1963) mapping in the Mahlangatsha area, it is suggested that the Mozaan strata have suffered at least three periods of deformation. The initial folding operated about axes directed east-northeast or north, while the final folding was along north-west axes, disrupting the original synclines into a series of centroclinal structures.

The data presented above clearly indicate that the Mozaan Group is intruded by granites of various types, and, as a result, has suffered metamorphism. Since the Witwatersrand Sequence overlies, and is not intruded by any of, the "Old Granites", it is difficult to see how the Pongola Sequence can be a correlative, unless:

1. there are various granites of different ages which are all included in the "Old Granites";
2. the Mozaan Group is a time-correlative of the Witwatersrand Sequence, but happens to be intruded by a younger granite in Swaziland and other areas.

Age determinations now appear to be in favour of the Pongola Sequence being considerably older than the Witwatersrand System. According to Nicolaysen et al (1962), the deposition of the Dominion Reef Group took place less than 3,050 m.y. ago. The Mozaan Group is intruded by a granite (G.4) which has an age of 3,070 m.y. (Allsopp et al, 1962). The G.4 age has been determined from four total rock analyses using the Sr/Rb method, the rock specimens being widely spread over Swaziland. No granites directly in contact with the Mozaan sediments have been dated so far. The assumption has to be made that the intrusive contact granites are the same as the dated G.4 granite.

If this assumption is valid, then the Pongola Sequence cannot be a time-correlative of the Witwatersrand Sequence. However, Davidson (1965), using an age of + 3070 m.y. for the Mozaan, stated that the age of the Witwatersrand and Dominion Reef rocks was the same, since the two rock groups had been correlated by the South African Geological Survey.

C. AIMS OF THE PRESENT INVESTIGATION

From the previous section, it is apparent that no satisfactory data exist to clarify the problem of the Upper Pongola (Mozaan) being a possible correlative of the Witwatersrand Sequence. As a possible approach to solving the problem, the present investigation was aimed at establishing, beyond doubt, the relationships of the G.4 and G.5 granites to the Mozaan sediments. In order to do this, the structural geological history of the supracrustal rocks in relationship to the granites had to be established. This involved determining relative-time relationships between folding, metamorphism, and, as it turned out, the time of intrusion of the two granites. Once the time relationships had been established, the next phase of the work was to determine the absolute ages of the granites in the contact area. This work was done in co-operation with the National Physical Laboratory of the Council for Scientific and Industrial Research in Pretoria.

Systematic field work in the area was started in April, 1963, and was completed in September, 1963. Several subsequent visits were made to the area, in order to clear up certain problems and to collect large (\pm 60 lbs.) specimens for age determinations. Mapping was carried out on 1:10,000 aerial photographs, and observations were transferred by means of a sketch-master to a base map of approximately the same scale. The latter was obtained from enlarging the existing topo-cadastral maps of Swaziland. The completed geological maps were then reduced to their present size for publication.

A total of 1081 minor structures was measured, of which 763 were of schistosity. Bedding, although visible on aerial photographs and distant outcrops, is by no means clear on a mesoscopic scale. Only 168 measurements of this element were made. Other minor structures measured included 67 of axial planes, 74 of fold axes and lineations, and nine of direction of tectonic transport derived from a plane containing deformed lineations and associated axial planes. Petrofabric analysis was first attempted on one of the G.4 granite specimens. The orientation of quartz grains was determined, but the petrofabric diagrams proved to be uninterpretable. Biotite proved more amenable. Specimens were then collected from three localities in the G.4 granite and one locality in the G.5 granite. In general, thin-sections were cut perpendicular to the dominant foliation plane in the granite, when this was present. The G.5 granite is exceptionally coarse, and 10 different slides had to be cut from a single specimen, to permit the measurement of only 87 biotite grains. However, the results were sufficiently diagnostic to be used. All petrofabric data have been restored to geographical co-ordinates, in order to compare with the minor structural data.

THE METAMORPHIC ROCK ASSEMBLAGE

The area mapped represents only a small portion of a regional map prepared by Winter (1963) (Figure 1). Since the stratigraphic and lithological detail of the rock types was investigated by Winter, this aspect was not restudied. Petrography has mainly been used to establish the grade of metamorphism, and to relate the time of metamorphism to the period of granite intrusion and tectonism.

A. METAMORPHOSED INSUZI ROCKS

The Insuzi Group is located in the western part of the map area (Figure 2). In general, rocks belonging to this Group develop poor outcrops, and are soil-covered. Locally, rounded boulder-like outcrops are found, while drainage gulleys give rise to the best exposures. The most common rock type is a massive dark green lava with amygdales. Hard chert-like felsitic varieties, which often reveal a foliation on weathered surfaces, are present in places. Intercalated with the massive type are lavas containing high concentrations of amygdales, porphyritic lavas, volcanic breccias, and scoriaceous bands. The outcrops are not good enough to establish a rigorous stratigraphic column in this area. However, two very useful marker horizons are present. One is a knotted schist consisting of porphyroblasts of andalusite lying in a matrix of quartz, andalusite, and pyrophyllite, the three last-mentioned minerals varying considerably in their relative proportions. Diaspore and damourite are also associated with this rock, occurring as veinlets or small lenses conforming generally to the main foliation (Davies et al., 1964). Above this aluminous-rich horizon, a ferruginous shale is found. The other phyllite horizon shown on the map (Figure 2) is light brown in colour, and has been particularly sensitive to deformation, containing abundant minor structures.

The stratigraphy is as follows :

- (5) generally amygdaloidal lavas, with some felsitic types.
- (4) upper phyllite band, rich in alumina.
- (3) massive felsitic lavas.
- (2) lower green phyllite, intensely folded.
- (1) amygdaloidal, porphyritic, and massive felsitic lavas,
with local intercalations of shale, scoriaceous
horizons, and volcanic breccia.

Under the microscope, it is quite clear that some of the lavas are completely metamorphosed. The amygdaloidal lavas consist of amphibole (tremolite-actinolite), biotite, epidote, chlorite, and quartz. Locally, remnant plagioclase phenocrysts can be recognized, but are in such a high state of alteration that petrographic identification is impossible. The felsites are essentially crypto-crystalline, though, locally, acid plagioclase phenocrysts are present. Other types consist of an equigranular fine-grained mosaic of quartz and mica (sericite and biotite), the mica showing a distinct preferred orientation. Blastoporphyritic remnant felspar grains are sometimes found in these rocks.

B. METAMORPHOSED MOZAAN ROCKS

The Mozaan rocks consist essentially of a sequence of metamorphosed quartzites, conglomerates, and shales. In the field, most of these rocks reveal a pronounced tectonic fabric which, in places, is highly complex, due to the superimposition of various phases of deformation originating under differently oriented stresses. However, certain quartzites reveal no visible fabric at all. They are generally pure quartzites, and differ from the other varieties which are charged with phyllosilicates. Schists, often with andalusite, have been derived from the metamorphism of shales. The sillimanite-bearing schist occurring in the eastern part of the area is also a particularly important marker band.

The conglomerate bands have been particularly useful in elucidating the structure. The scattered pebble conglomerate zone shown in the centre of Figure 2 emphasizes this point. The lowermost conglomerate band is characterized by the presence of pebbles and boulders larger in size than any of the other conglomerates. In the southern part of the area the following sizes were observed : 18" x 5", 9" x 6", 11" x 7", 13" x 5". The

central scattered pebble conglomerate zone shows considerable macroscopic variation in pebble concentration, but well-developed conglomerates have not been observed. Pebble sizes vary between $\frac{1}{4}$ " and 6" in diameter. Locally, the pebbles show a distinct flattening in the main ($S_1 - S_2$) tectonic fabric plane. The matrix of the conglomerate is essentially fine-grained quartz and sericite, while the pebbles are of quartz. The other conglomerate horizons of the area vary in width from several inches to several feet. In general, the pebble size is of the order $\frac{1}{2}$ " - 2" in diameter, though, locally, larger pebbles up to 6" in diameter are found. The pebbles consist entirely of quartz, while the matrix is composed of quartz and sericite. Reddish varieties contain iron oxides and hydroxides. Under the microscope, yellowish-green tourmaline and zircon have been observed, in addition to the opaque minerals.

The quartzites reveal gradations from pure meta-quartzites, free of impurities, to mica-quartz schists. The higher the sericite content, the more pronounced the planar and folded fabric. In general, these rocks consist of two major components, quartz and sericite, with accessory tourmaline, zircon, and opaque minerals of several varieties. Under the microscope, the quartz produces an even-grained mosaic with interlocking grains, individuals of which often reveal a pronounced elongation in the main S_1 or S_2 fabric planes in the purer quartzites (Figure 3). Micaeous varieties have a distinct preferred orientation (and often also concentration) of mica flakes in the main S_1 or S_2 fabric planes. Where these planes have been folded in certain localities, the quartz grains are noticeably reduced in size, suggesting a certain amount of cataclastic action associated with the post $S_1 - S_2$ folding. As the granite contacts are approached in the east, the mineral sillimanite makes its appearance in some of the more aluminous quartzites. It is often associated with muscovite, and is itself developed as fine-grained fibrolite. The impure quartzites become quartz-muscovite (sericite) and quartz-muscovite-sillimanite assemblages.

Towards the base of the Mozaan succession, several metamorphosed shale horizons are exposed. These rocks comprise dark knotted phyllites, with andalusite nodules occurring in varying degrees of concentration. In some hand specimens, characteristic chiastolite crosses can be observed. The average grain-size of the andalusite is $\frac{1}{8}$ " - $\frac{1}{4}$ ". Microscopically, the andalusite has a porphyroblastic texture, the surrounding fine-grained matrix wrapping itself around this mineral. Porphyroblasts are commonly altered to a very fine-grained phyllosilicate mass (pyrophyllite ?), with remnant highly anhedral andalusite occurring at the centre of the altered grain, indicating retrogressive metamorphism. Similar effects are found in the matrix of quartz, sericite, and chlorite. Chloritoid is scattered throughout the rock as small tabular grains, sometimes preferentially developed in altered andalusite porphyroblasts which have larger concentrations of adjacent chlorite. It would appear that an original assemblage of quartz-andalusite-chlorite-muscovite altered to quartz-pyrophyllite-chlorite-sericite-chloritoid. Chloritoid possibly indicates higher stresses than were present during the earlier metamorphism, the mineral occurring in an area where S_3 folds are particularly well developed.

C. SIGNIFICANCE OF THE METAMORPHIC ASSEMBLAGES

The lower grades of metamorphism give rise to the following assemblages:-

- (a) quartz + (albite) + tremolite-actinolite + zoisite + biotite + chlorite
- (b) andalusite + pyrophyllite
- (c) quartz-andalusite-chlorite-muscovite

Between rocks with these mineral assemblages and the higher-grade varieties are quartz-sericite schists with no index mineral apart from muscovite. Near the granite contact, the stable assemblage is quartz-sillimanite-muscovite. The diagnostic minerals, andalusite and

sillimanite, suggest a facies series of the Abukuma-type of metamorphism (Miyashiro, 1961; Winkler, 1965). The lower grade schists would belong to the greenschist facies, and the sillimanite schists to the cordierite-amphibolite facies. The presence of chloritoid in some of the knotted schists probably indicates retrogressive metamorphism under a higher stress gradient than that of the Abukuma-type facies series.

In the adjacent area to the south, staurolite has been recorded by Winter (1963). Approximately 30 miles still further to south, where an identical stratigraphical sequence is intruded by granite of presumably the same age, the mineral kyanite is developed (Humphrey and Krige, 1931). This indicates either that a uniform geothermal gradient was not active over the different areas, or that later periods of folding during the same thermal event had varying stress gradients associated with them. It is also possible that the type of metamorphism passed very close to the triple point of andalusite, kyanite, and sillimanite.

Miyashiro (1961) has pointed out that the Abukuma facies series need not necessarily be developed on a regional scale, but may be representative of a localized contact metamorphism caused by synkinematic intrusions. This condition prevails in the Mahlangatsha area. Kennedy (1960) has shown that pyrophyllite is stable up to 600°C at a pressure greater than 4 kilobars, provided that the water pressure is equal to the rock pressure. With lower water pressures sillimanite and quartz or kyanite and quartz will form. Within the Mahlangatsha area it must be accepted that pyrophyllite is stable in the metamorphosed Insuzi sequence. Closer to the granite the association sillimanite and quartz and sillimanite and kyanite and quartz are stable, which may indicate that the water pressure was lower than the rock pressure in the Mozaan sediments undergoing metamorphism.

THE INTRUSIVE GRANITES AND DYKES

The area mapped (Figure 2) contains only the G.5 granite (Hunter, 1961). The disposition of this granite clearly reveals that it is discordant and intrusive into the Insuzi and Mozaan rocks. Figures 1 and 4 show that the structures are cut off by the granite, and that the general plunge of the northerly syncline, defined by the scattered pebble conglomerate, is down into the granite. The quartzites adjacent to the granite exhibit intense recrystallization. Towards the southeast of the area (Figure 1), Winter (1963) has shown that the G.4 granite intrudes and metamorphoses the Mozaan sediments. Several samples of the granite were taken from this contact for petrofabric and petrographic studies, the localities of the samples being shown in Figure 1.

A. THE G.4 GRANITE

This granite is grey and medium-grained in texture. Close to its contact with the Mozaan rocks, the granite is often banded, containing biotite-rich lenses up to several inches in width (Figure 5). Pegmatite lenses have been observed near the large dolerite body occurring in the southern part of Figure 1. A distinct foliation caused by a pronounced orientation of mica is observable close to the contact. Near the G.5 granite, the G.4 variety becomes noticeably coarser in grain size, and loses its microscopic planar fabric. It would appear, therefore, that the G.5 granite has influenced and recrystallized the G.4 granite.

Under the microscope, the granite is composed essentially of felspar, quartz, biotite, and green hornblende. The felspars constitute approximately 60 per cent of the rock, and consist of microcline perthite and turbid oligoclase. Smaller plagioclase grains are often included in the microcline perthite. The biotite is a greenish-brown variety which alters to chlorite and epidote. Apatite is found in minute euhedral grains, often concentrated together.

concentrated together with biotite, although it may also be associated with the other minerals. Pleochroic haloes in the micas surround small zircon grains. Zircon also occurs as isolated rare grains in other constituents. Allanite, a rare constituent, appears as rather altered large grains, yellowish-brown in colour, with euhedral outlines. Sphene is scattered throughout the rocks in small amounts as discrete grains, tending to develop euhedral outlines, and altering to a white opaque mass of leucoxene. Green hornblende is found in some varieties as subhedral grains which alter to chlorite and epidote. Rare grains of pyrite are disseminated through the rock.

B. THE G.5 GRANITE

This granite contrasts markedly with the above type. It is pink, coarse-grained, and porphyritic, individual potash felspar phenocrysts being up to 1 inch in diameter. It is markedly homogeneous as regards texture and composition. No visible fabric can be detected, the potash felspar phenocrysts and biotite being apparently randomly oriented. From field inspection, it would seem to conform to a typical high-level granite.

Microscopically, the rock reveals the presence of microcline, orthoclase, oligoclase, quartz, biotite, sphene, and allanite. The microcline is characterized by the development of two distinct varieties of perthite. One is an extremely fine and regular combination of patch and film perthite, while the other, although showing a general preferred orientation, consists of irregular veinlets branching, swelling and often cross-cutting the main trend of film perthite. The oligoclase is generally turbid, and is frequently bordered by a zone relatively free of inclusions. Myrmekitic textures are found at some margins of the plagioclase grains, particularly where in contact with potash felspar grains. The biotite is a strongly pleochroic variety, varying in colour from yellowish-green to dark greenish-brown. It is often associated with tabular apatite grains and larger altered euhedral allanite crystals. The biotite also contains small inclusions of zircon. On altering, the biotite changes to chlorite and epidote. Scattered throughout the rock are large subhedral sphene grains.

C. ZIRCONS FROM THE GRANITES

One 70 lb. sample of each granite was collected from the localities B and D shown in Figure 1. The samples were crushed, and the heavy minerals concentrated, using a Wilfley table, Franz isodynamic separator, and heavy liquids. Two final concentrates of zircon were obtained which have been used for age determinations. Representative samples from these were mounted on glass slides for morphological and size investigations. The slides were traversed by means of a movable stage attached to a Swift point counter. The characteristics of each intersected zircon were recorded until a total of 200 euhedral crystals was obtained from each sample. In the case of the G.5 granite, 516 grains had to be examined before 200 euhedral crystals were found, while with the G.4 variety only 360 had to be studied. The G.5 granite had a significantly higher proportion of broken grains than the G.4 type.

The characteristics of the zircons from the different granites are shown in Table 1. Several features are significant. The G.5 zircons are generally bigger, and show a greater range of size and form. The regression line used to fit the length-breadth plots; i.e. the reduced major axis (R.M.A.), shows that the zircons from each granite belong to significantly different populations. A plot of the R.M.A. for the two different granites is shown in Figure 6. Length frequency plots are shown in Figure 7. Here, again, it can be seen that the G.4 granite zircons are limited to a particular length ratio (0.1 - 0.2), while there is a wider spread in the corresponding data from the G.5 granite, pointing to a wider range of shapes. The reason for the differences in zircon shapes and elongation ratios may be twofold:

TABLE 1

Granite	% Zoned	% Overgrown	No. of Grains
G.4	14.5	20.0	360
G.5	9.5	6.0	516

Zoning and Zircons with Distinct Cores

	% Prismatic elongate types	% Equidimensional types	% Broken Individuals	% Anhedral types	% Composite types
G.4	53	4	25	16	2
G.5	30	11	35	21	3

General Morphological Characteristics

	Mean Length \bar{x} (mm.)	Std. Dev. of Length S_x (mm.)	Mean Breadth \bar{y} (mm.)	Std. Dev. of Breadth S_y (mm.)	Slope S_y/S_x ^a	Std. Error of Slope	Correl. Coefft. between x and y	Relative Dispersion about R.M.A.
G.4	0.1547	0.0402	0.0723	0.0149	0.03706	0.012	0.6466	0.6?
G.5	0.1940	0.0789	0.0900	0.0364	0.4614	0.021	0.7220	14.0

Reduced Major Axis Data (after Larsen and Poldervaart, 1957)

1. the G.4 zircons were nucleated on pre-existing zircons (higher proportion of overgrown types), and the shape of earlier zircons influenced the subsequent shapes that were attained during granite consolidation; this would imply that the G.4 granite was not entirely magmatic;

2. the G.5 granite was truly magmatic, and at the time of zircon development less restriction was imposed on growth rates in particular crystallographic directions.

Figure 8 shows some typical zircons from the two granites.

D. DYKES

Figure 2 shows certain large faults which traverse the area. These invariably contain relatively high-grade kaolin deposits at certain localities which are soil covered. D. Hunter has kindly supplied the author with drill cores of material underlying this kaolin zone which occurs in the dyke. The material underlying the kaolin consists of a reddish fragmentary rock, rich in clay minerals, quartz, and hematite. Below this, "dyke-rock" has been encountered. The latter is obviously a metamorphosed product consisting of a fine-grained mixture of green amphibole, epidote, quartz, and chlorite. In hand specimen, a porphyritic texture is suggested, the phenocrysts now being represented by aggregates of phyllosilicate and epidote. These were probably felspar phenocrysts which have been metamorphosed. The dyke-material that filled the fault zones is thus pre-metamorphic in age. A recent paper by Hunter and Uri (1966) explains the origin of the kaolin deposits.

STRUCTURAL GEOLOGY

A. MAJOR STRUCTURES

The major structures found in the map area are best understood by referring to Figures 2 and 4. In the west, the Insuzi lava sequence dips towards the east, and, in turn, is overlain by Mozaan sediments which are truncated to the north and east by granite. If the geological map is studied conjointly with the map showing strike and dip measurements of bedding (Figure 4), then it is clear that the area is very broadly synclinal. The synclinal structure is well defined by a zone of scattered pebble conglomerates occurring in the central part of the map area. The lava sequence is not repeated on the eastern side of the syncline, because of the occurrence of intrusive granite which is obviously discordant with respect to the structure.

The central syncline is more complex than would appear on first examination. It is divided by a cross-cutting anticlinal fold which splits the syncline into two major portions, the northern part plunging to the north, and the southern part to the south. These major structures strike approximately north-south, while the cross-folds appear to have a northeast strike, as can be judged from the outcrop pattern depicted in Figure 9. Further evidence of this cross-folding is suggested by the outcrop pattern near the hinge region of the southern syncline, where another smaller cross-fold is present (Figure 9).

A very complex fold pattern occurs in the eastern part of the map area where the sillimanite-bearing quartzite appears. Here, a north-south striking subsidiary anticline is apparently related to the major synclinal trend. The northern part of the structure is further complicated by cross-folding.

B. ANALYSIS OF DATA ON MINOR STRUCTURES

(a) Bedding

The orientation of bedding planes is shown in Figure 4. The synclinal nature of the structure is well defined by the scattered pebble conglomerate zone. Less data are present for the hinge zone of the northward plunging syncline than for the southward plunging structure.

A composite plot of all the bedding plane data is shown in Figure 10. Two separate great circles fit the data representing pi-pole girdles for the two synclines. This was tested by plotting the data from each syncline separately. Because of the quality of the

data, the great circle pi-plot for the southward plunging syncline is more reliable than for the northern syncline which gives an elongate maximum, in contrast to the spread revealed by the other structure. From this data, it can be deduced that the northern syncline plunges at 15° on a bearing of 8° , while the southern syncline plunges at 25° on a bearing of 205° . Both structures appear to be relatively open, this being due to the fact that the actual trough of the hinge zone is exposed.

(b) Axial Plane Cleavages

(i) S_1 and S_2 Folding

Occurring over the whole area is a very pronounced, steeply dipping schistosity. This is particularly noticeable in some of the more impure quartzites, and is produced by a parallel alignment and rude concentration of sericite in distinct planes. Pure quartzites may also reveal a faint type of foliation on outcrop surfaces, this being due to the parallel elongation of quartz grains during metamorphism. This fabric is, by far, the most common in the area, also being found in the various types of phyllite. About the only rocks which do not macroscopically display this fabric are the lavas. However, even here, some of the weathered surfaces of the felsites portray this planar fabric.

The orientation of this structure within the mapped area is shown in Figure 11. There is, however, a complicating factor. At four localities in the mapped area, the schistosity in the quartzites has been refolded about new folds, the axial planes of which are closely aligned to the original cleavage. For this reason, all the schistosities have been classed together as S_1 and S_2 , since both may be present but cannot be distinguished. There is, however, good evidence that two phases of folding are present (Figure 12). On examination of Figure 13, it can be seen that the S_1 and S_2 schistosities have a northerly strike in the northern part of the area, but become rotated into a northeasterly trend in the central part of the area where they are affected by the northeast fold trend. The schistosities are thus rotated by younger fold trends.

The $S_1 - S_2$ schistosity trend is associated with the major synclines in the area, having formed synchronously with these folds. This may be deduced from the fact that, in the stereographic projection of the poles to the cleavages, the maximum lies on the pi-girdle defined from the bedding plane data (Figures 10 and 14). This is particularly true in the case of the northward plunging syncline, whence most of the data are derived. The stereographic projection (Figure 14) merely defines a very steeply dipping cleavage which has been slightly rotated by later movements (a spread over approximately 70° on the periphery of the projection), and which has an average orientation of : strike 90° — dip generally vertical.

(ii) S_3 Folding

At some localities, a post- $S_1 - S_2$ schistosity is found. This is particularly well illustrated in the hills lying immediately to the south of the anticlinal divide separating the two major synclines (Figures 11 and 13). In this area, the $S_1 - S_2$ and a younger schistosity can be seen making a small angle with each other. They are often very difficult to distinguish from each other. In this area, where the $S_1 - S_2$ schistosity is regionally bent into a more northeasterly direction, the younger S_3 schistosity is straight and undeformed, while the $S_1 - S_2$ schistosity shows local folding. This confirms the observations on a larger scale shown in Figure 11, where the $S_1 - S_2$ cleavage exhibits rotation. A stereographic plot of the poles to these schistosities defines an average orientation of : strike 45° ; dip vertical (Figure 15). They thus differ significantly from the main $S_1 - S_2$ trend.

This cross-fold trend is responsible for the refolding of the original north-south-trending syncline occurring in the centre of the map area, which has resulted in the formation

of the anticline between the two synclines plunging in opposite directions.

* (iii) S₄ Folding

The orientation of the axial planes, associated cleavages, and lineations of this period are shown in Figure 16. The characteristic feature is the non-development of any major folds. The deformation must have been fairly intense in certain places because, locally, in impure quartzites, good schistosities have been produced. The minor structures related to this period occur over the whole area, in contrast to the S₃ fabric which is confined to a fairly narrow zone.

The dominant minor structures are cleavage-schistosity, very fine micro-folds, minor folds, and (S₁ - S₂) - (S₄) cleavage intersections. The time of formation of this fabric can be fairly well established. There are numerous examples of these folds deforming the S₁ - S₂ foliation (Figure 18). The same appears to hold for the S₃ foliation, though no definitive examples could be found in the field. Another strong argument in favour of a post-S₃ age is the conspicuous single maximum obtained on the stereographic plot of the cleavage and axial planes of these folds (Figure 17). Had there been any S₃ deformation after the flat folds, then the S₄ fold data from the northern syncline would be separable on the stereoplot from that of the southern syncline. That this is not the case means that the S₄ structures were superimposed on the already bent S₁ - S₂ syncline. The average orientation of the S₄ cleavages and axial planes is : strike 56°; dip 30° towards the northwest. Figure 17 also shows the plot of lineations associated with this folding. These all lie in the axial plane, confirming the superimposed nature of this fold trend.

At three different localities, the "a" kinematic axes of this period of deformation could be determined on lineated quartz veins folded by the S₄ structures, using the method of Ramsay (1960). The lineations were imprinted on the quartz veins during the S₁ - S₂ period of folding, so that some of the quartz veins at least were formed prior to the earliest deformation. The three "a" kinematic axes determined are shown in Figure 19 with respect to the average orientation of the axial plane of the S₄ period. An approximate orientation of the "a" axis is : strike 315°; plunge 32° to the north-northwest.

(iv) S₅ Folding

A peculiar feature of the area is that, in certain localities, all the above fabrics become deformed in, and adjacent to, planes which represent the original bedding (Figure 20). During the previous periods of folding, the bedding surfaces remained passive, but during S₅ times they were reactivated. Within the bedding planes a new fabric was formed, which is parallel to the original bedding. In places the fabric is intense, and above and below it the earlier fabrics are clearly bent in a systematic manner, indicating differential movement on the bedding plane surfaces (Figure 20). The width of these zones measures from several inches to several feet. Within the wider zones, the earlier cleavages and local quartz veins show distinct folding. The folding is destructive, as it leads to a pronounced reduction in grain size, shredding of original quartz veins, and the complete obliteration of the original foliation (see Figure 21).

It is concluded that the bedding planes and some of the more incompetent horizons acted as detachment surfaces along which thrust movements took place after the formation of the S₄ schistosity. The displacement is invariably such that upper horizons moved relatively westwards. This direction has been determined from outcrop profiles where the differential movement can be clearly seen, and is thus a general direction only. The development of this bedding plane shear is at an optimum in the northern part of the area, and was used as such to determine the strike and dip of the original bedding.

(c) Time Relationships of Metamorphism and Folding Phases

It appears that the major period of metamorphism slightly preceded, and was also synchronous with, the S_1 - S_2 foliation. Using porphyroblasts, as suggested by Zwart (1960, 1962), and their relationships to the S_1 - S_2 structures, two situations are revealed :

(i) The foliation appears to have been formed after the andalusite porphyroblasts, as demonstrated by the porphyroblast containing no S_1 trails and the foliation being compressed around the more competent grain (Figure 22a and b). The andalusite itself is highly altered to pyrophyllite, so that the metamorphism at the time of the S_1 - S_2 foliation formation may be retrogressive at certain localities. Figures 22a and b also suggest that "pressure shadows" form in the foliation direction, next to the andalusite porphyroblasts. Here, they often reveal highly frayed margins, and there is an obvious enrichment of quartz in the schistose matrix. This again suggests the earlier development of the andalusite.

(ii) Figure 23 shows the congruency of the S_1 trails in the andalusite, and the S_1 - S_2 schistosity defined by sericite. Here, the andalusite formed during S_1 - S_2 folding.

Where sections have been cut perpendicular to the S_2 fold axes, originally aligned micas have been rotated by the S_2 folds (Figure 12). Thus, the original fabric may have formed in the S_1 period of deformation. Some of the metamorphosed argillaceous quartzites have sillimanite grains lying with their long axes in the S_1 - S_2 foliation plane. This may indicate that the sillimanite formed together with, or after, the S_1 - S_2 foliation. By far the most common rock types are quartz-sericite-schists. The schistosity is formed by mica grains having parallel orientation. Here again the micas define the S_1 - S_2 fabric plane. Some of the purer quartzites that show a visible fabric in hand specimens reveal an interlocking mosaic of quartz grains under the microscope, the long axes of the quartz grains lying in the fabric plane (Figure 3). The recrystallization was again associated with the S_1 - S_2 period. There is thus ample evidence to show that the metamorphism of the area took place together with the earliest S_1 and S_2 deformations, and that some of the metamorphism was even earlier. Certain evidence is in support of the earliest metamorphism and planar fabric formation having taken place in the S_1 fold period (Figure 12).

That the other fold periods (S_3 and S_4) deformed the original metamorphic fabric can be demonstrated by examining thin-sections cut normal to either S_3 or S_4 lineations. The earlier S_1 and S_2 planar fabric is clearly folded, and is, in places, re-oriented into new planes, with a certain amount of recrystallization (Figures 24, 25, and 26).

The quartz in the reactivated bedding planes, along which thrust movements took place, generally shows a reduction in grain-size. The micas show recrystallization, in certain places, parallel to the shearing surfaces.

C. PETROFABRIC ANALYSES OF THE G.4 AND G.5 GRANITES

Three oriented specimens of G.4 granite were taken from localities A, B, and C in Figure 1, while one of G.5 granite was collected at locality D. The orientation of quartz grains in the G.4 granite could not be determined, but the blotites give rise to well-

defined girdles (Figures 27, 28, and 29). The mica flakes, when restored to their correct geographic orientation, show the following relationships:

1. The poles to the girdles all lie on a great circle (Figure 30).

2. The pole to this great circle is where the three biotite girdles intersect at a common point. This common point is significant, as it corresponds to a maximum occurring in the girdles which is common to at least two, and possibly three, of the girdles (Figure 30). This common maximum is identical to that of the poles to the axial plane cleavages of deformation S_4 (Figure 17). Thus, all three specimens contain micas which have been rotated about the S_4 axial plane. In short, an S_4 biotite orientation has been superimposed on the granite.

3. The other maxima in the girdles of Figures 28 and 29 correspond with the $S_1 - S_2$ maximum and the S_3 maximum, respectively (Figures 14 and 15). Thus, all the periods of deformation, with the exception of the S_5 period, can be identified in the biotite girdles of the G.4 granites.

4. The origin of these girdles is controlled by the original biotite orientation ($S_1 - S_2$ or S_3) and the later S_4 orientation. There is a tendency for the former to be rotated into the latter. The biotite girdle which is thus formed is the great circle passing through two biotite maxima (S_3 , or $S_1 - S_2$, and S_4 maxima), and which has its pole located on the great circle defined by the S_4 maximum (i.e., the average orientation of the cleavage associated with the S_4 period of deformation).

5. The specimen of G.4 granite lying closest to the G.5 granite (Figure 27) is noticeably coarser-grained, containing no visible fabric. The biotite girdle from this granite is not as well-defined, and shows a higher degree of dispersion in comparison with the girdles obtained from granites farther away from the G.5 contact (Figures 28 and 29). These features might well be related to a certain degree of metamorphism and recrystallization of the G.4 by the G.5 granite.

Petrofabric analyses were also carried out on the coarser-grained G.5 granite. Due to the coarseness of the rock, the orientation of only 87 biotites could be measured. The data are shown in Figure 31. Various statistical tests (Fairbairn, 1949) have not resolved whether the mica flakes are randomly or systematically oriented. However, when it is appreciated that a random distribution does not necessarily mean an even distribution of data on the stereo projection (Flinn, 1958), then the G.5 data could well be random. The maximum depicted in the diagram, if of significance, does not appear, upon rotation into the geographically correct orientation, to be related to any of the known fold trends.

An oriented specimen of G.4 granite, occurring 15 miles to the south-southwest of the area mapped, was also subjected to petrofabric analysis. Indications of the S_3 and S_4 effects were observed, showing that the deductions made for the structural history of the Mahlangatsha area are also valid elsewhere.

THE AGE OF THE PONGOLA SEQUENCE

U-Pb measurements, carried out in collaboration with the National Physical Research Laboratory of the C.S.I.R., have yielded minimum ages of 3,050 m.y. and 2,600 m.y. for the G.4 and G.5 granites, respectively. Whereas doubt could be expressed before as to the age of the Pongola Sequence, since no contact phase of the G.4 granite has been dated, these new data show that the Pongola rocks, as defined and developed in the Mahlangatsha area, are older than a 3,050-m.y. intrusive granite. Allsopp (1964) has

determined the following age limits to the Witwatersrand and Dominion Reef strata :

		<u>Uranium Mineral Ages (Detrital)</u> m.y.	<u>Maximum Sediment Ages</u> m.y.
Witwatersrand	:	2,980 ± 100	2,720 ± 100
Dominion Reef	:	3,100 ± 100	2,820 ± 100

These data show quite clearly the Pongola Sequence is, in fact, older than the basal Dominion Reef Group of the Witwatersrand Sequence. Its exact position in the time-scale of South African geology still remains to be determined, particularly with respect to the Swaziland Sequence which is also intruded by granites 3,000 m.y. old.

The G.4 granite has been affected by S_4 period of folding, and also contains evidence of the S_1 - S_2 and S_3 periods. From the work of Winter (1963), it is clear that the G.4 granite has intruded the Pongola rocks. Large fragments of Mozaan quartzite occur in the G.4 granite, being completely surrounded by it. These rocks, as well as those lying adjacent to the granite contact, contain such metamorphic minerals as sillimanite and staurolite (Winter, 1963). From the structural analysis, it has been established that the metamorphism was strongly influenced by the S_1 - S_2 fabric. Some metamorphic minerals grew before, and during, the formation of the fabric plane. This evidence shows that the G.4 granite was responsible for a heat gradient which gave rise to metamorphic minerals, but was also subject to the same deformative forces that affected the Pongola supra-crustal rocks. This granite is thus synkinematic, but differs from synkinematic granites developed in geosynclines. The latter are generally of anatetic origin, being found in areas affected by regional metamorphism, and show a high degree of concordancy with the surrounding rocks. Moreover, they are generally confined to the eugeosynclinal environment of an orogenic belt (Roering, 1967). In contrast, the G.4 granite is discordant, responsible for contact metamorphic phenomena, and intrusive into Pongola rocks. The latter comprise andesites (Hunter, 1961) and shallow-water sediments characteristic of a depository on a continent or a craton. The Mahlangatsha area thus reveals evidence of granites encroaching on the craton. Granites of the same age intrude supra-crustal rocks in the Barberton Mountain Land.

It can be concluded that, as far back as 3,000 m.y. ago, cratonic environments probably existed. Geosynclinal environments, such as the Barberton Mountain Land, also existed in these ancient times (Roering, 1967). The fact that large granite masses encroached on, and intruded, the craton is significant. Younger granitic bodies intruded into epeirogenic environments are related to subvolcanic phenomena, and, in comparison to the G.4 granite, are of minor extent. It is suggested that granite activity of a type similar to the G.4 variety may be directly related to some fundamental fractional process in the mantle. It is thus strongly contrasted to granite developed in mobile belts, which are largely anatetic and confined to active zones of intense metamorphism in such belts. The older-type granites are possibly directly responsible for the formation of the crust, and their significance is possibly less apparent, due to a diminished frequency of exposure as a result of thickening of the crust, in younger geologic time where granitic phenomena are directly related to the mobile belts.

From a viewpoint of structural geology, it is interesting to note that many of the deformational fabrics developed (S_1 to S_4) in the supra-crustal rocks are also reflected in biotite orientations in the G.4 granite. No readily visible fabrics are present in many of the hand specimens, but the petrofabric studies have permitted a distinction being made between Precambrian granites of different age. The G.4 granite is synkinematic and the G.5 post-kinematic.

* * * * *

LIST OF REFERENCES CITED

- Allsopp, H.L., Roberts, H.R., Schreiner, G.D., and Hunter, D.R. 1962 Rb-Sr Age Measurements on Various Swaziland Granites. *Journ. Geophys. Res.*, Vol. 67, p. 5307-5313.
- Allsopp, H.L. 1964 Rubidium-Strontium Ages from the Western Transvaal. *Nature*, Vol. 204, p. 361-363.
- Davidson, C.F. 1965 The Mode of Origin of Banket Orebodies. *Bull., Inst. Mining Metall.*, Vol. 74, p. 319-338.
- Davies, D.N., Urié, J.G., Jones, D.H., and Winter, P.E. 1964 The Alumina, Pyrophyllite and Silica Deposits in the Insuzi Series, Mahlangatsha and Mkopeleli Area, Shiselweni and Manzini Districts. *Bull. No. 4, Swaziland Geol. Survey*, Mbabane, p. 5-22.
- Du Toit, A.L. 1931 Explanation : Sheet 109 (Nkandhla). *South African Geological Survey*, Pretoria.
- Fairbairn, H.W. 1949 Structural Petrology of Deformed Rocks (Second Edition). Addison-Wesley Press, 344 pp.
- Flinn, D. 1958 On Tests of Significance of Preferred Orientation in Three-Dimensional Fabric Diagrams. *Journ. Geology*, Vol. 66, p. 526-539.
- Hall, A.L. 1918 The Geology of the Barberton Gold Mining District. *Memoir No. 9, South African Geological Survey*, Pretoria.
- Hamilton, G.N. 1938a The Geology of the Country Around Kubuta (Southern Swaziland). *Trans., Geol. Soc. S. Afr.*, Vol. 41, p. 41-82.
- Hamilton, G.N. 1938b Further Notes on the Geology of the Country Around Kubuta. *Trans., Geol. Soc. S. Afr.*, Vol. 41, p. 199-203.
- Humphrey, W.A., and Krige, L.J. 1931 The Geology of the Country South of Piet Retief : An Explanation of Sheet No. 68. *South African Geological Survey*, Pretoria.
- Hunter, D.R. 1957 The Geology, Petrology, and Classification of the Swaziland Granites and Gneisses. *Trans., Geol. Soc. S. Afr.*, Vol. 60, p. 85-120.

- Hunter, D.R. 1961 The Geology of Swaziland.
Swaziland Geological Survey, Mbabane.
- Hunter, D.R. 1963 The Mozaan Series in Swaziland.
Bull. No. 3, Swaziland Geological Survey,
Mbabane, p. 5-16.
- Hunter, D.R., and Urié, J.G. 1966 The Origin of Kaolin Deposits, Mahlangatsha,
Swaziland.
Economic Geology, Vol. 61, p. 1104-1114.
- Kennedy, G.C. 1960 Phase Relations of Some Rocks and Minerals
at High Temperatures and High Pressures.
Trans., Amer. Geophys. Union, Vol. 41,
p. 283-286.
- Larsen, L.H., and
Poldervaart, A. 1957 Measurement and Distribution of Zircons in
Some Granitic Rocks of Magmatic Origin.
Mineralogical Magazine, Vol. 31, p. 544-564.
- Matthews, P.E. 1959 The Metamorphism and Tectonics of the Pre-
Cape Formations in the Post-Ntingwe Thrust
Belt, S.W. Zululand, Natal.
Trans., Geol. Soc. S. Afr., Vol. 62,
p. 257-322.
- Mehliss, A.T.M. 1961 The Geology of the Portion of the Country
Between Mankalana and Hlatikulu, Mankalana
District, Swaziland.
Bull. No. 1, Swaziland Geological Survey,
Mbabane, p. 36-55.
- Miyashiro, A. 1961 Evolution of Metamorphic Belts.
Journ. Petrology, Vol. 2, p. 277 ff.
- Nicolaysen, L.O., Burger, A.J., 1962 Evidence for the Extreme Age of Certain
and Liebenberg, W.R. Minerals from the Dominion Reef Conglomerates
and the Underlying Granite in the Western
Transvaal.
Geochimica et Cosmochimica Acta, Vol. 26,
p. 15-23.
- Ramsay, J.G. 1960 The Deformation of Early Linear Structures in
Areas of Repeated Folding.
Journ. Geology, Vol. 68, p. 75-93.
- Roering, C. 1967 Non-Orogenic Granites in the Archean Geo-
syncline of the Barberton Mountain Land.
Information Circular No. 35, Economic
Geology Research Unit, University of the
Witwatersrand, Johannesburg.
- Truter, F.C. 1949 A Review of Volcanism in the Geological History
of South Africa.
Proc., Geol. Soc. S. Afr., Vol. 52,
p. xxix - lxxxix.

- Truter, F.C., and Rossouw, S. 1955 Gravity Map of the Union of South Africa,
South African Geological Survey, Pretoria.
- Winkler, H.G. 1965 Petrogenesis of Metamorphic Rocks.
Springer Verlag, Berlin, 220 pp.
- Winter, P.E. 1963 Unpublished Departmental Report.
Swaziland Geological Survey, Mbabane.
- Zwart, H.J. 1960 Relations Between Folding and Metamorphism
in the Central Pyrenees, and their Chronological
Succession.
Geologie en Mijnbouw, Vol. 22, p. 163-180.
- Zwart, H.J. 1962 On the Determination of Polymetamorphic
Mineral Associations, and its Application to the
Bosost Area (Central Pyrenees).
Geologische Rundschau, Vol. 52, p. 38-65.

* * * * *

KEY TO FIGURES

- Figure 1 : Regional geological map of the Mahlangatsha area.
- Figure 2 : Geological map of the northern part of the Mahlangatsha plateau.
- Figure 3 : Relatively pure quartzite showing quartz grain elongation in the main
 S_1 - S_2 fabric plane. Crossed-nicols. 65x magnification.
- Figure 4 : Map showing the orientation of bedding planes.
- Figure 5 : Banding in G.4 granite. Scale in cms.
- Figure 6 : Reduced major axis plot of zircons from the G.4 and G.5 granites.
- Figure 7 : Length frequency diagrams of zircons from G.4 and G.5 granites.
- Figure 8 : Characteristic zircon types from the G.4 and G.5 granites.
- Figure 9 : Major structural trends based on the outcrop pattern and bedding plane
orientations.
- Figure 10 : Plot of poles to bedding planes. 158 observations. Data defines two
folds : one plunges at 15° on bearing of 80° , second plunges at 25° on
bearing of 205° .
- Figure 11 : Map showing the orientation of steeply-dipping schistosities.
- Figure 12 : Thin-section cut perpendicular to S_2 fold axis. An original (S_1) sericite
foliation has been rotated about an S_2 fold axis. 65x magnification.

- Figure 13 : Generalized strike directions of S_1 - S_2 schistosity and S_3 schistosity. Regional bending of S_1 - S_2 trend by constant S_3 trend.
- Figure 14 : Poles to the S_1 - S_2 schistosity. 434 observations. Average orientation of schistosity : bearing 90° , dip vertical. Circle represents one of the maxima in the biotite girdle developed in the G.4 granite (from Figure 28).
- Figure 15 : Poles to S_3 schistosity. 41 observations. Average orientation of schistosity : bearing 45° , dip vertical. Circle represents one of the maxima in the biotite girdle developed in the G.4 granite (from Figure 29).
- Figure 16 : Map showing the orientation of shallow-dipping axial planes, schistosities, associated minor fold axes, and lineations.
- Figure 17 : Poles to S_4 schistosity (small dots). 168 observations. Average orientation of schistosity : bearing 56° , dip 30° NNW. Large dots represent the orientation of associated lineations. Circle represents one of the maxima which is present in the biotite girdles of three different G.4 granite specimens.
- Figure 18 : Sericite-quartz schist. Original S_1 - S_2 foliation defined by sericite flakes which have been bent by S_4 folds. 65x magnification.
- Figure 19 : Deduced "a" tectonic axes (dots) of the S_4 deformation, shown in relation to the average orientation of the S_4 schistosity (determined from Figure 17).
- Figure 20 : The relationship of the S_5 movement planes (original bedding) to the earlier deformational planar fabrics (S_1 - S_2 and S_4). All diagrams are approximately east-west sections looking southwards.
- Figure 21 : Quartz vein folded and sheared by S_5 thrust movements in an argillaceous quartzite horizon.
- Figure 22 : Altered porphyroblasts of andalusite represented by fine-grained phyllosilicate (pyrophyllite ?) and quartz. The matrix of the rock is essentially quartz, sericite, and chlorite. Schistosity compressed on porphyroblasts, and the enrichment of quartz on one side of the altered grain, suggestive of a "pressure-shadow", both indicate that the porphyroblast probably was pre-tectonic. Crossed-nicols. 40x magnification.
- Figure 23 : Andalusite (dark) in which Si-trails conform with the schistosity in the matrix, which is defined by the parallel orientation of the sericite. The matrix consists of quartz and sericite. Crossed-nicols. 65x magnification.
- Figure 24 : Sericite-chlorite-quartz schist with chloritoid. The original S_1 - S_2 foliation has been deformed by a later S_4 folding. The development of a new S_4 cleavage is apparent. 65x magnification.
- Figure 25 : Sericite-chlorite-quartz schist with andalusite (large, dark grey individual). Original S_1 - S_2 fabric in matrix and andalusite deformed by S_4 folds. 65x magnification.
- Figure 26 : Sericite-quartz schist. Original S_1 - S_2 cleavage deformed by S_4 fold.

- Figure 27 : Biotite girdle obtained from G.4 granite at locality A in Figure 1. Data rotated into correct position occupied by specimen in field, 200 measurements. Contoured at 1, 2, and 3 per cent.
- Figure 28 : Biotite girdle obtained from G.4 granite at locality B in Figure 1. Data rotated into correct position occupied by specimen in field, 200 measurements. Contoured at 1, 2, 3, 4, and 8 per cent.
- Figure 29 : Biotite girdle obtained from G.4 granite at locality C in Figure 1. Data rotated into correct position occupied by specimen in field, 200 measurements. Contoured at 1, 2, 3, 5, and 8 per cent.
- Figure 30 : Synthesis of data from Figures 27, 28, and 29. Poles to established girdles represented by dots. The great circle containing these poles has its pole lying in one of the maxima found in the individual girdles. Solid black contour from Figure 28, dashed contour from Figure 29, dotted contour from Figure 27, in which one of the lobes coincides with this position.
- Figure 31 : Petrofabric diagram of 87 biotites from the G.5 granite at locality D in Figure 1. N. azimuth corresponds to reference line on original specimen. The "maximum" in the lower southern part of the diagram bears no relationship to any of the established trends when rotated to the position the specimen occupied in the field.
- Figure 32 : Biotite orientations of G.4 granite occurring 15 miles to the SSW. of the Mahlangatsha area. 130 measurements. Contours at 1, 2, 3, 4, 5, 6, and 7 per cent. A similar pattern to Figure 29 is revealed.

* * * * *

FIG.1

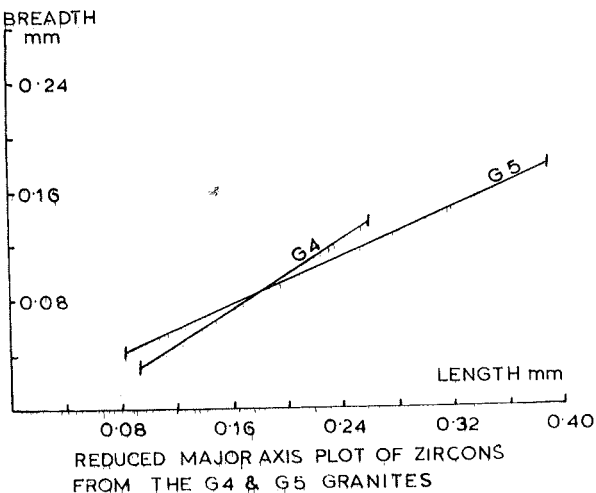
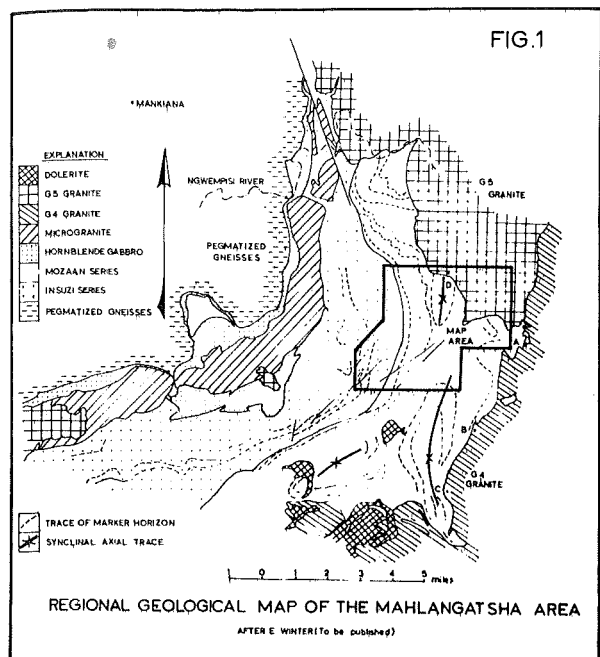


FIG.6

FIG.7

LENGTH FREQUENCY DIAGRAMS OF
ZIRCONS FROM THE G4 AND G5
GRANITES

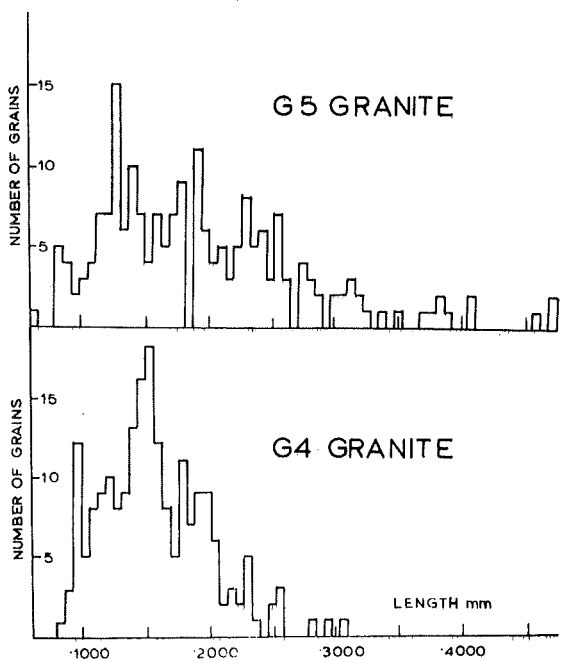


FIG.9

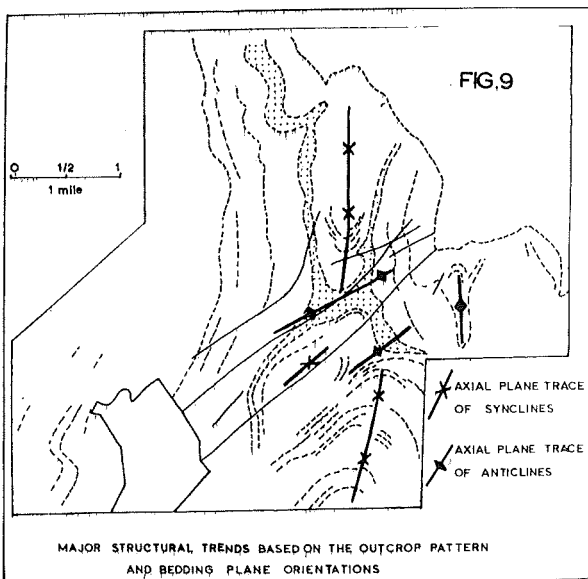
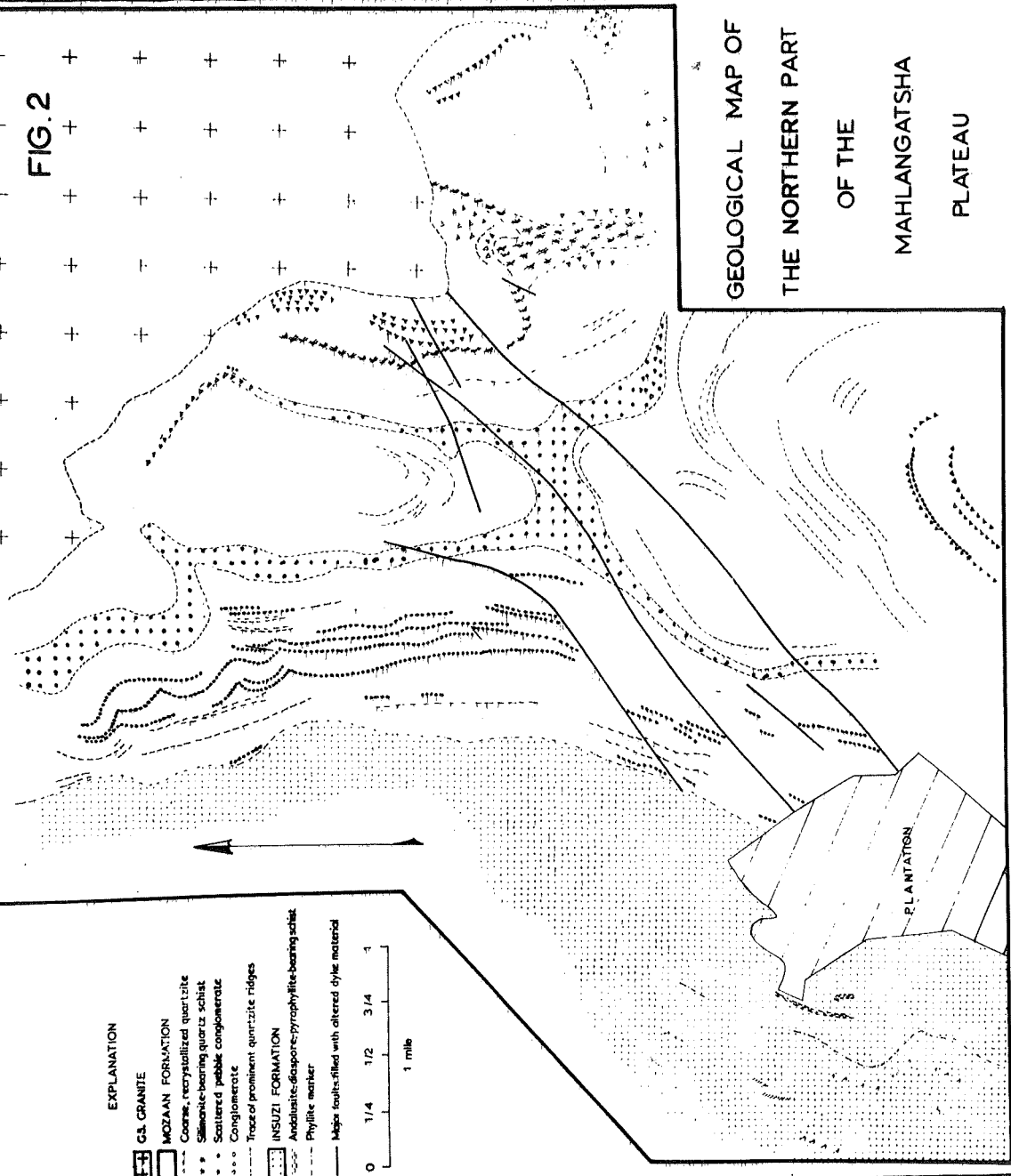


FIG. 2

GEOLOGICAL MAP OF
THE NORTHERN PART
OF THE
MAHLANGATSHA
PLATEAU



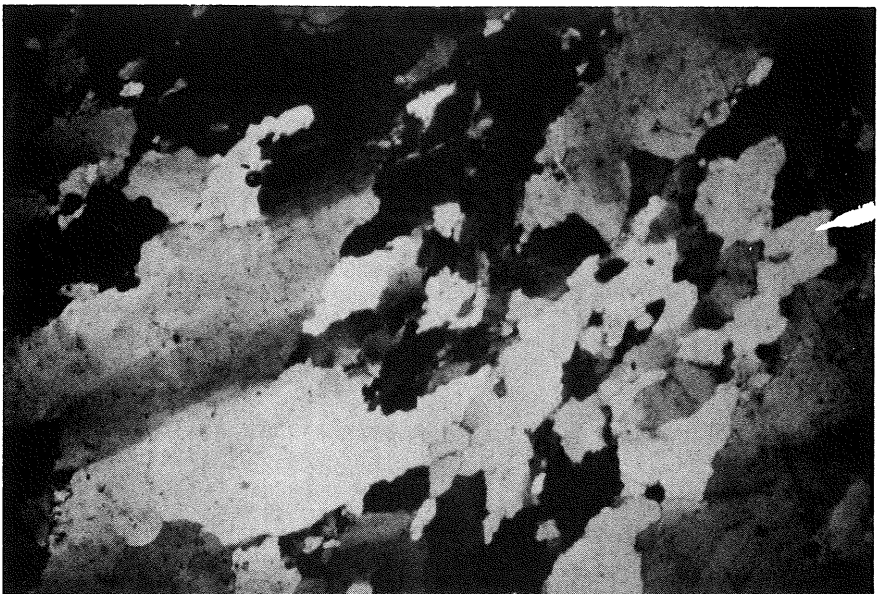


FIG. 3

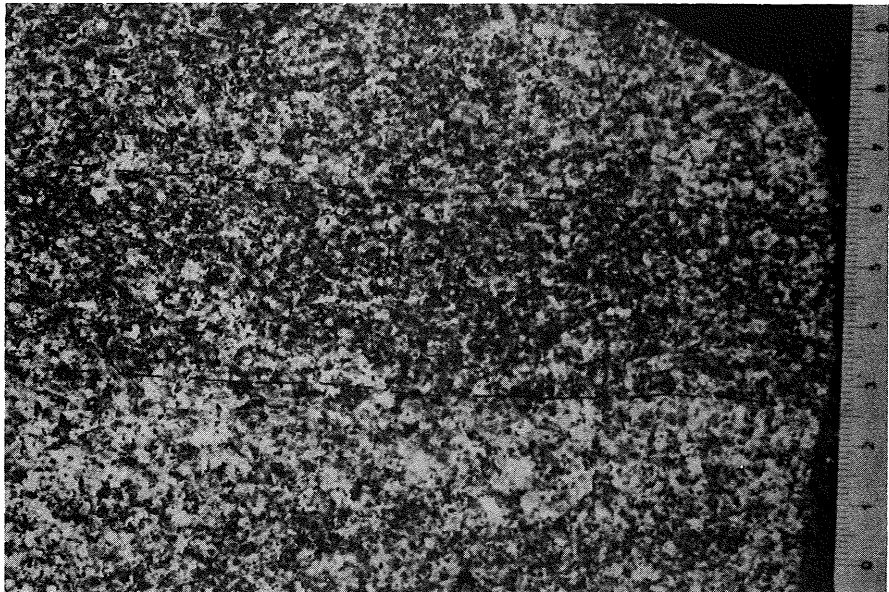


FIG. 5

FIG. 4

MAP SHOWING
THE ORIENTATION OF
BEDDING PLANES

DIRECTION OF STRIKE AND
AMOUNT OF DIP

26

1/4 1/2 3/4 1

0 1/4 1/2 3/4 1
1 mile

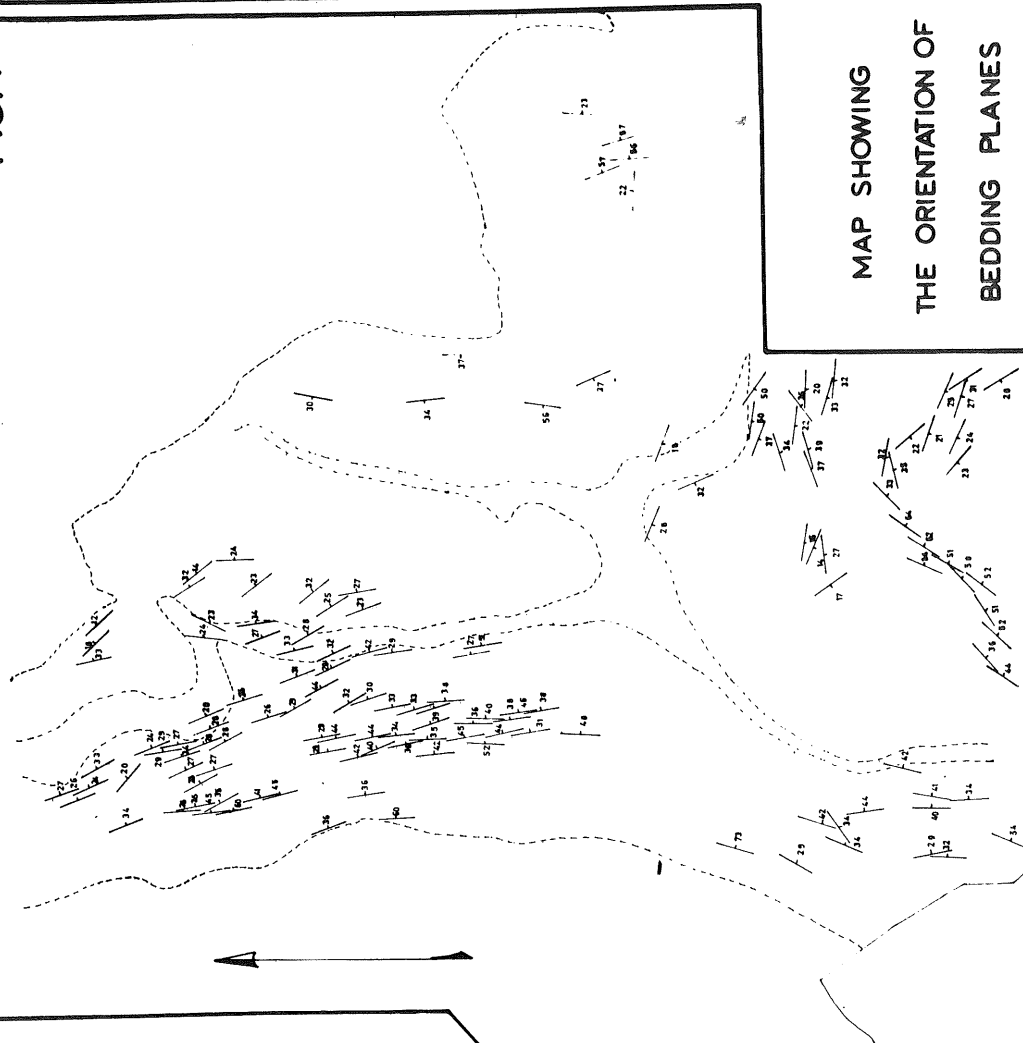
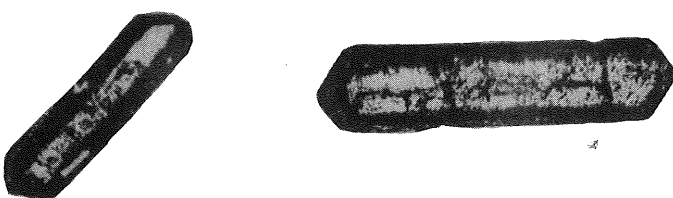
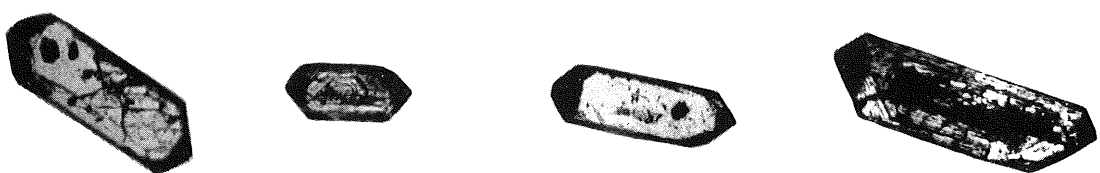


FIG 8



G 4



G 5

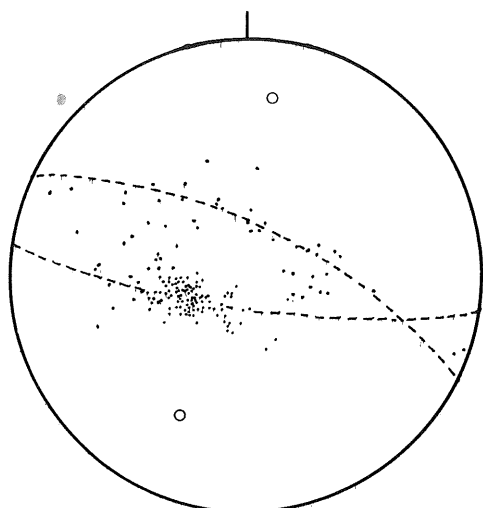


FIG.10

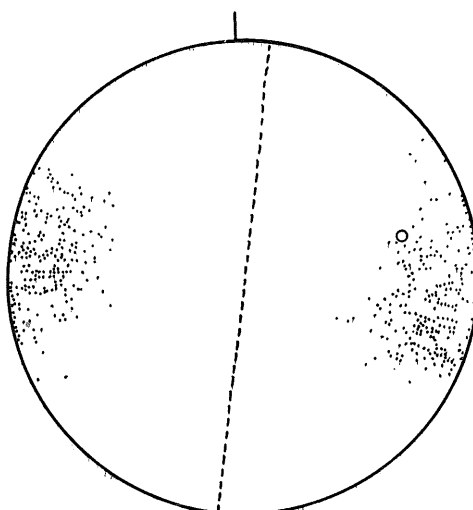


FIG.14

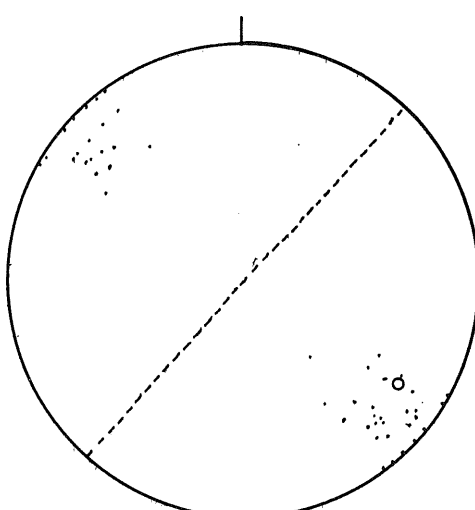


FIG.15

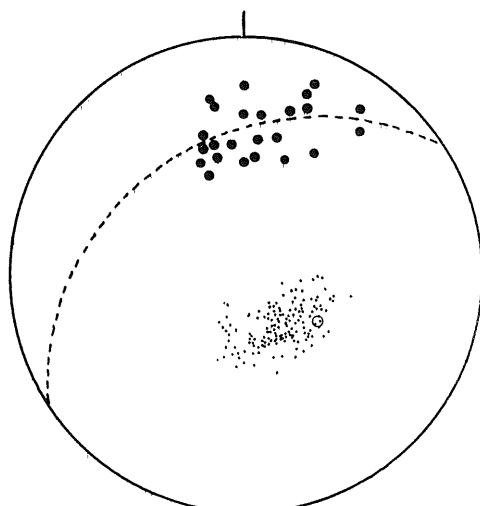
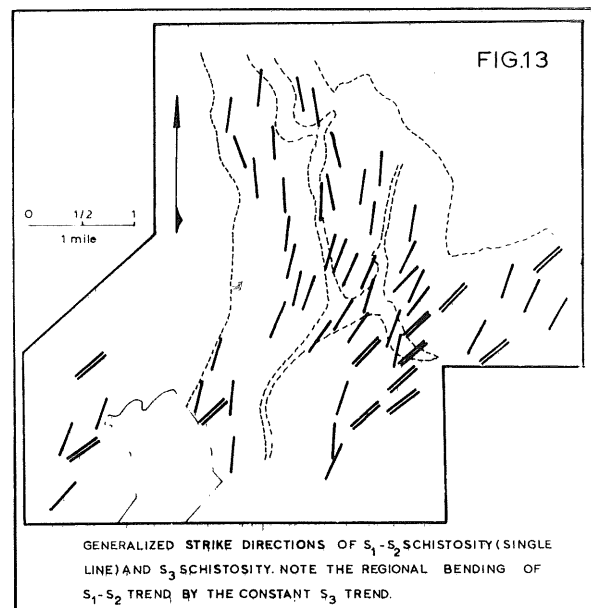


FIG.17

FIG.11

EXPLANATION

- DIRECTION OF STRIKE AND DIP
- VERTICAL DIP
- $S_1 \& S_2$ SCHISTOSITIES
- S_2 SCHISTOSITY
- S_3 SCHISTOSITY

0 $\frac{1}{4}$ $\frac{1}{2}$ $\frac{3}{4}$ 1
1 mile

MAP SHOWING THE
ORIENTATION
OF
STEEPLY DIPPING
SCHISTOSITIES

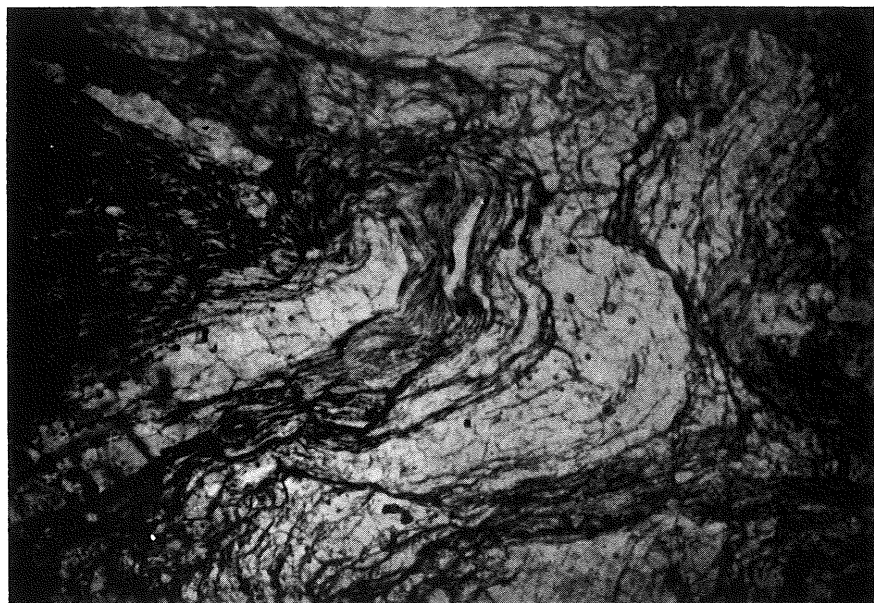


FIG.12



FIG.18

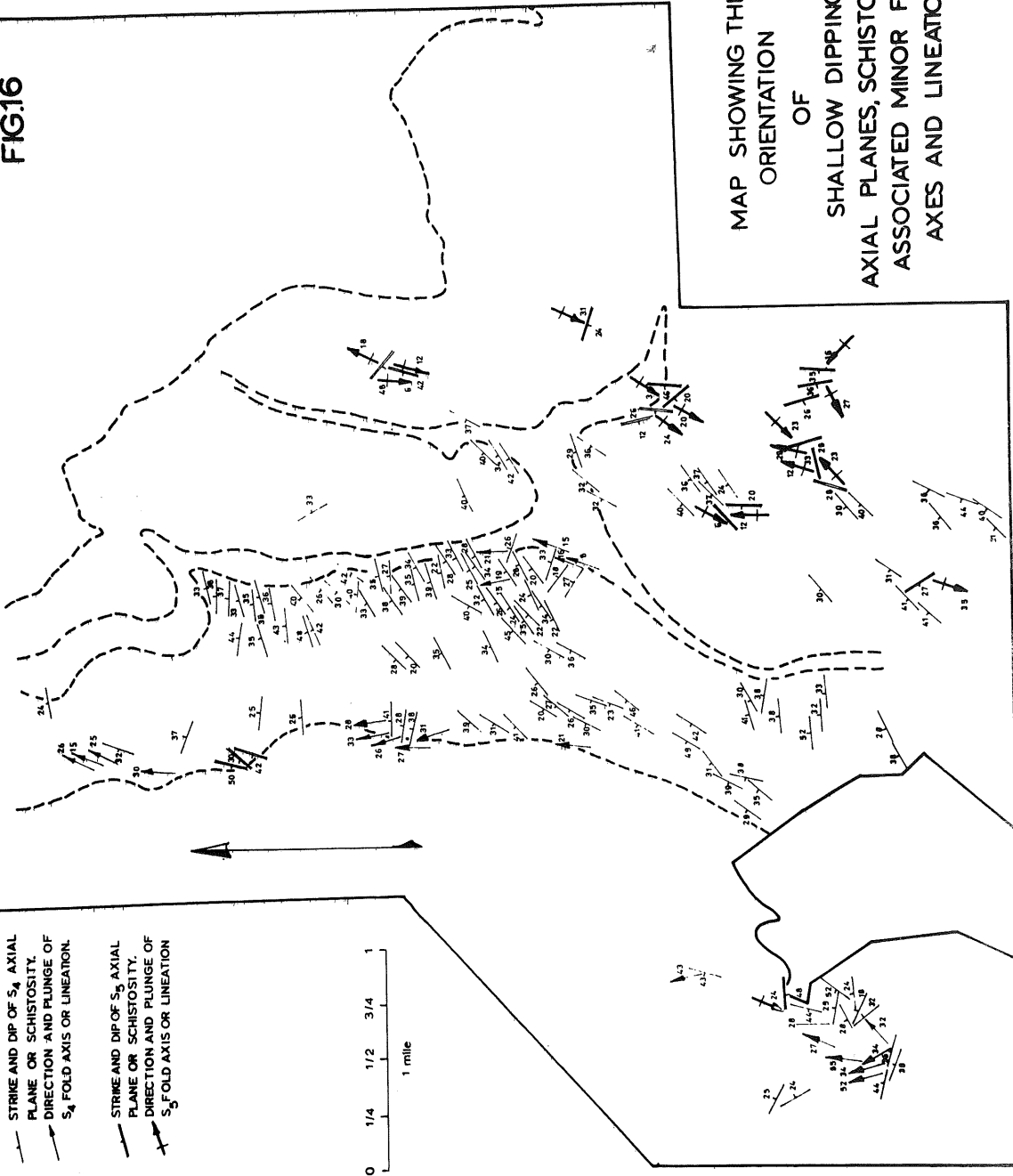
EXPLANATION

- STRIKE AND DIP OF S_4 AXIAL PLANE OR SCHISTOSITY.
- DIRECTION AND PLUNGE OF S_4 FOLD AXIS OR LINEATION.
- STRIKE AND DIP OF S_5 AXIAL PLANE OR SCHISTOSITY.
- DIRECTION AND PLUNGE OF S_5 FOLD AXIS OR LINEATION

0 1/4 1/2 3/4 1
1 mile

FIG.16

MAP SHOWING THE ORIENTATION OF SHALLOW DIPPING AXIAL PLANES, SCHISTOSITIES, ASSOCIATED MINOR FOLD AXES AND LINEATIONS



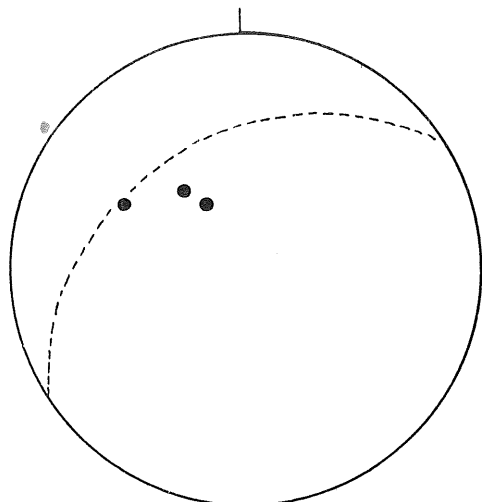


FIG. 19

SHOWING THE RELATIONSHIP OF THE S_5 MOVEMENT PLANES (ORIGINAL BEDDING) TO THE EARLIER DEFORMATIONAL PLANAR FABRICS (S_1-S_2 & S_4).
ALL DIAGRAMS ARE APPROXIMATE EAST-WEST SECTIONS LOOKING SOUTHWARDS.

FIG. 20

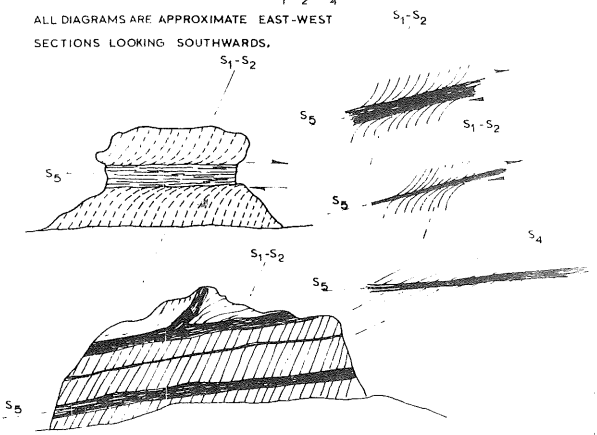


FIG. 21

QUARTZ VEIN FOLDED AND SHEARED BY
 S_5 THRUST MOVEMENTS IN AN ARGILLA-
CEOUS QUARTZITIC HORIZON

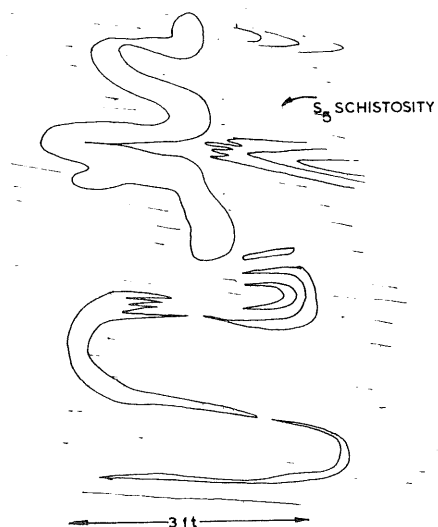


FIG. 27

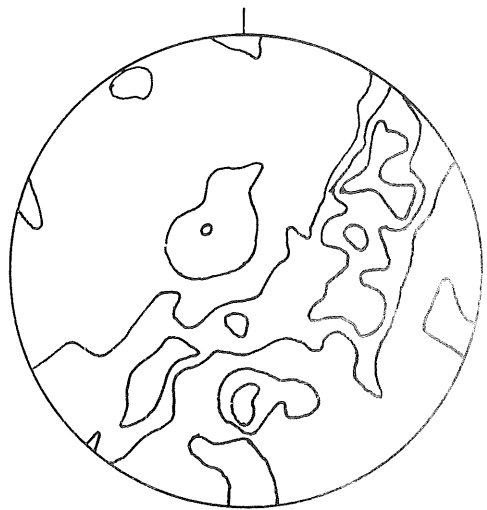
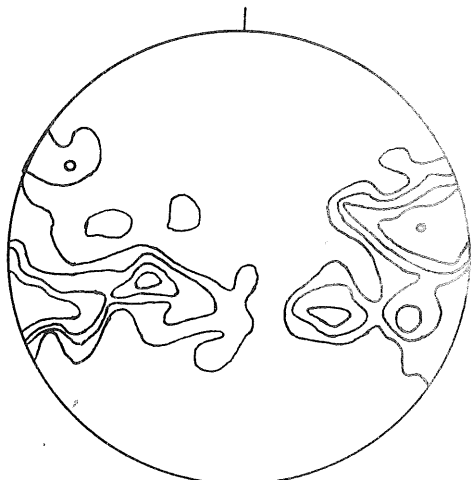


FIG. 28





a



b

FIG.22

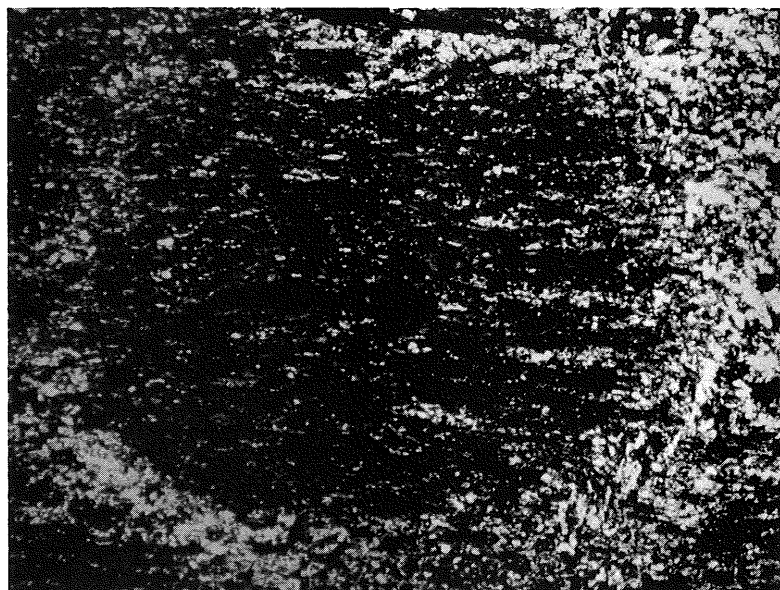


FIG.23

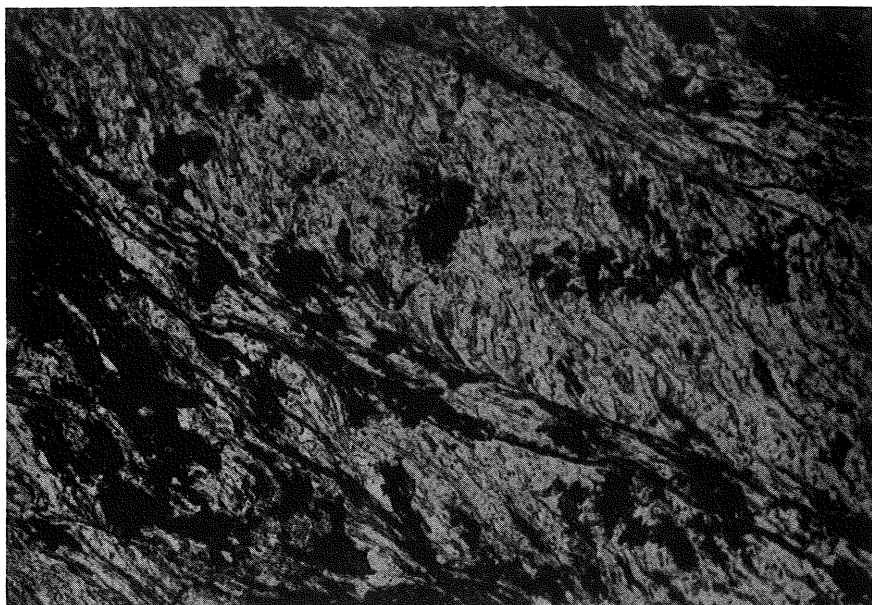


FIG.24

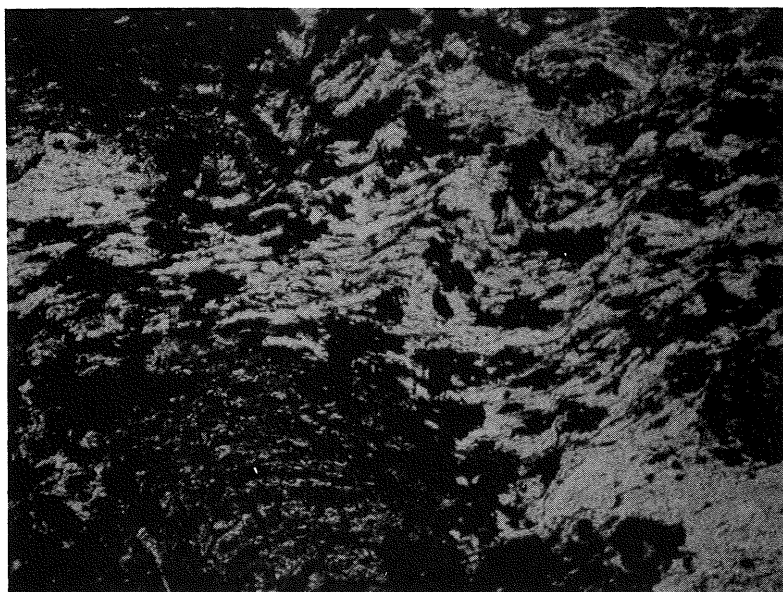


FIG.25

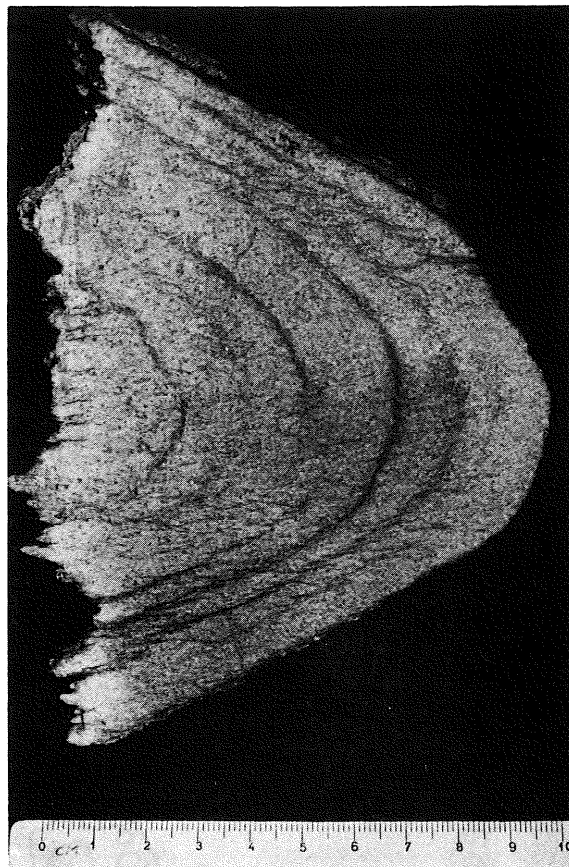


FIG. 26

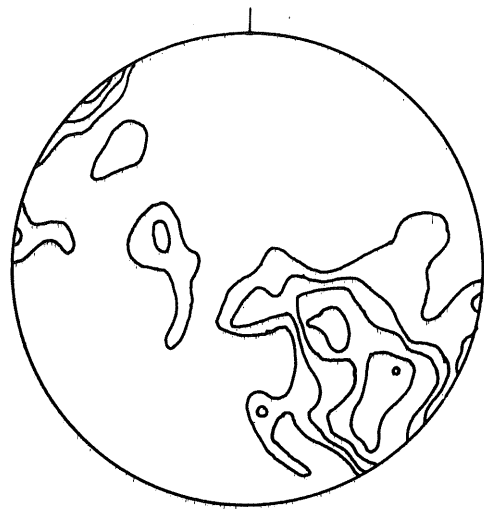


FIG. 29

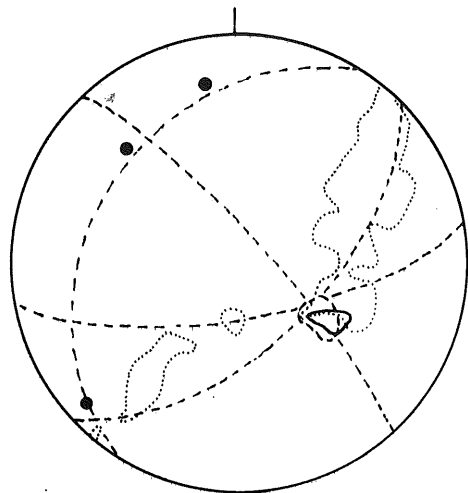


FIG. 30

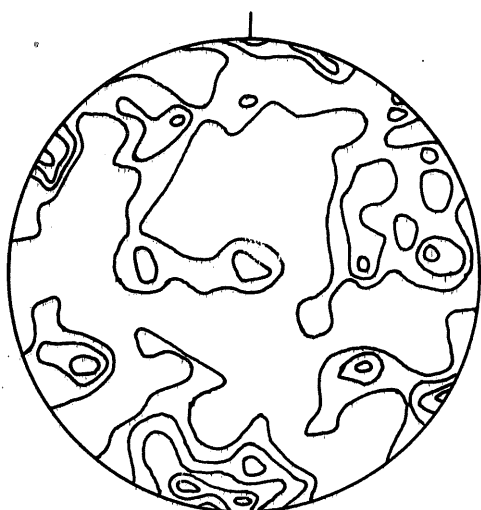


FIG. 31

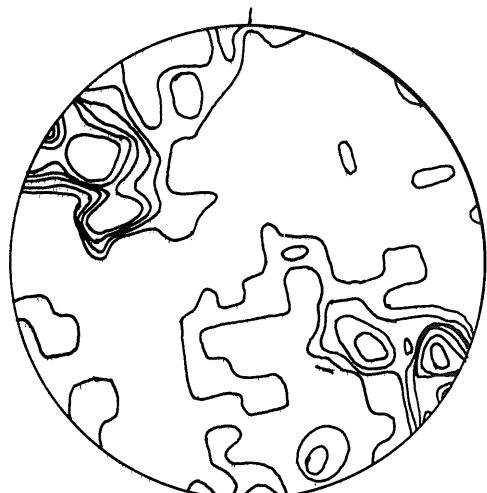


FIG. 32